PNAS

Supplementary Information for

Extracellular Matrix Physical Properties Govern the Diffusion of Nanoparticles in Tumor Microenvironment

Xiaocong He[a,b#], Yuanyuan Yang[a,b#], Yulong Han[c#], Chunyu Cao[a,b], Zhongbin Zhang[a,b], Lingxiao Li[a,b], Cailan Xiao[d], Hui Guo[e], Lin Wang[f], Lichun Han[g], Zhiguo Qu[h], Na Liu[d*], Shuang Han[i*], Feng Xu[a,b*]

[a] *The Key Laboratory of Biomedical Information Engineering of Ministry of Education, School of Life Science and Technology, Xi'an Jiaotong University, Xi'an 710049, P.R. China*

[b] *Bioinspired Engineering and Biomechanics Center (BEBC), Xi'an Jiaotong University, Xi'an 710049, P.R. China*

[c] *State Key Laboratory of Mechanics and Control of Mechanical Structures Nanjing University of Aeronautics and Astronautics, Nanjing 210016, P. R. China*

[d] *Department of Gastroenterology, The Second Affiliated Hospital of Xi'an Jiaotong University, Xi'an 710049, P.R. China*

[e] *Department of Medical Oncology, The First Affiliated Hospital of Xi'an Jiaotong University, Xi'an 710061, P.R. China*

[f] *Engineering Research Center of Personalized anti-aging health product development and transformation, College of medicine, Xi'an International University, Xi'an 710077, Shaanxi, China*

[g] *Department of anesthesia, The Xi'an Daxing Hospital, Xi'an 710049, P.R. China*

[h] *Key Laboratory of Thermo-Fluid Science and Engineering of Ministry of Education, School of Energy and Power Engineering, Xi'an Jiaotong University, Xi'an 710049, P.R. China*

[i] *Department of Gastroenterology, HongHui Hospital, Xi'an 710054, P.R. China*

[#] *Authors contributed equally*

[*] *Corresponding authors:*

liuna1@xjtu.edu.cn; shuanghamy@163.com; fengxu@mail.xjtu.edu.cn

This PDF file includes:

Materials & Methods

Figs. S1 to S8

Tables S1 to S4

Captions for Movies S1 to S4

References for SI reference citations

Other supplementary materials for this manuscript include the following:

Movies S1 to S4

Materials & Methods

1. The vascularity characterization of tissues

The tissue immunohistochemical (IHC) staining was performed with an anti-CD31 antibody (Abcam, UK) according to the instructions of the IHC kit (ZSGB-BIO, China). IHC results were determined based on staining intensity and proportion of positive cells.

2. Experiments of NPs diffusion in collagen hydrogels

2.1 Collagen hydrogels with different concentrations

Considering that NPs traditionally used for tumor treatment have a typical size range from 30 nm to 100 nm, we investigated the diffusion of mesoporous silica NPs (Qiyue Biotechnology Co., Ltd, China) with size of approximately 50 nm in collagen hydrogels. The morphology of the NPs was revealed in TEM images (**Fig. S3a**). The NPs were covalently labeled with rhodamine isothiocyanate (RITC).

NP penetration in collagen hydrogel was performed in μ-slide channels (ibidi, Cat#80606) as previously reported [1]. Rat tail collagen I was added to a centrifuge tube placed in an ice bath, followed by the addition of deionized water. Then the mixture was added to 0.2 mol/L NaOH solution and mixed immediately. Then the 10× PBS was added and fully mixed to form the final mixture with a final collagen I concentration of 0.7 mg/mL, 1.0 mg/mL and 1.5 mg/mL, respectively. μ-slide channels were pre-cooled on ice and 30 μL of the above mixture was pipetted into each channel through one reservoir. Then the μ-slide was placed in a 37 ℃ incubator for 50 min for collagen assembly.

To track the penetration of fluorescent NPs, 30 μL of the RITC-labeled NPs was added into one of the reservoirs for each channel while the reservoir on the other side was added with 30 μL of 1× PBS. Then the μ-slide was placed in the 37 ℃ incubator for 2 h for NP diffusion into the collagen hydrogel with different concentrations. Confocal fluorescent imaging was performed at 20× magnification by scanning a 1024×1024 pixel (636.4×636.4 μm) ROI of the center line of channel at the edge of the reservoir. Confocal reflectance mode was also used to characterize the collagen morphology and density simultaneously.

Confocal fluorescent images were analyzed using ImageJ to assess the NP diffusion in collagen I hydrogels. To develop the intensity-penetration depth profile for each collagen concentration, mean fluorescence intensity of the brightest area (a 180×10 pixel ROI at the direction of high NP concentration) of each image was regarded as the reference intensity. Mean fluorescence intensity of three 20×20 pixel ROIs was measured and averaged at each fixed penetration depth and normalized to the reference intensity. Diffusion coefficients (D) were calculated by fitting intensity-penetration depth profile to standard 1-D analyte diffusion equation (1).

$$C(x,t) = A\,erfc\left(\frac{x}{2\sqrt{Dt}}\right) \quad (1)$$

2.2 Collagen hydrogels with different stiffness

To form glycated stiffer collagen, collagen stock solution was mixed with ribose in 0.02M acetic acid to containing a final concentration of 0 or 100 mM ribose and incubated at 4°C for 5 days. Then collagen was neutralized and gelled to obtain a final concentration of 3 mg/mL as described above.

2.3 Collagen hydrogels with different structures

For NP diffusion in collagen network and aligned collagen, collagen I mixtures were prepared firstly on ice with a final concentration of 3.0 mg/mL. Then the final mixture was injected into a home-made rectangular mold with a length of 1.5 cm, a width of 0.8 cm and a depth of 500 μm. And ~15 iron oxide particles with diameter of ~100 μm were embedded in both ends of the collagen solution mixture in the mold, followed by gelation in a 37 ℃ incubator for 1 h. After gelation, collagen hydrogels encapsulating iron oxide particles were gently detached from the mold and transferred to a petri dish. The collagen hydrogel structure obtained was original with randomly distributed fibers. Then a small amount of 1× PBS was added into the petri dish until the collagen hydrogel was submerged. To prepare aligned collagen, two magnets were placed under both ends of the obtained collagen to stretch the collagen until the length of the collagen reached 1.7 cm. After 24 h, magnets and excess liquid were removed and the aligned collagen was obtained. Finally, a

volume of 30 μL RITC labeled mesoporous silica NPs was injected into the two kinds of collagen hydrogels carefully. Collagen hydrogels with NPs were placed in the 37 ℃ incubator for 6 h for NP diffusion. Fluorescence distribution was observed using CLSM and images were captured at the edge of injected sites. Confocal reflectance mode was also used to characterize the collagen morphology.

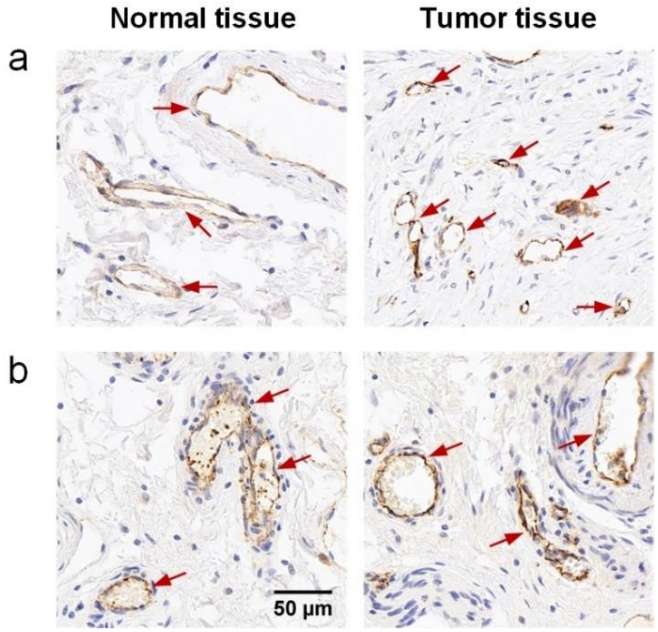

Fig. S1. The vascularity characterization of the tumor and normal tissues from IHC staining. a, Normal and tumor tissues with disparate vascularity. **b,** Normal and tumor tissues with similar vascularity. Vessels are marked with red arrows in all subgraphs.

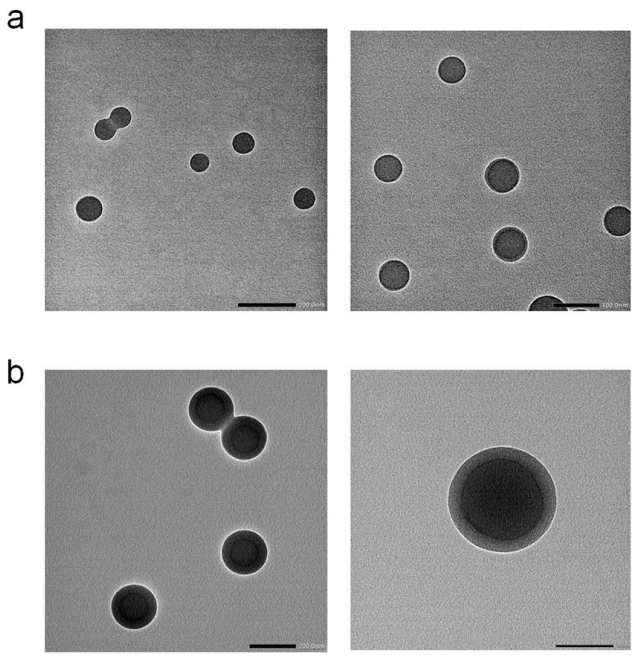

Fig. S2. Characterization of polystyrene (PS) NPs. a, TEM images show the morphology of the NPs with a diameter of approximately 80 nm. **b,** TEM images show the morphology of the NPs with a diameter of approximately 200 nm.

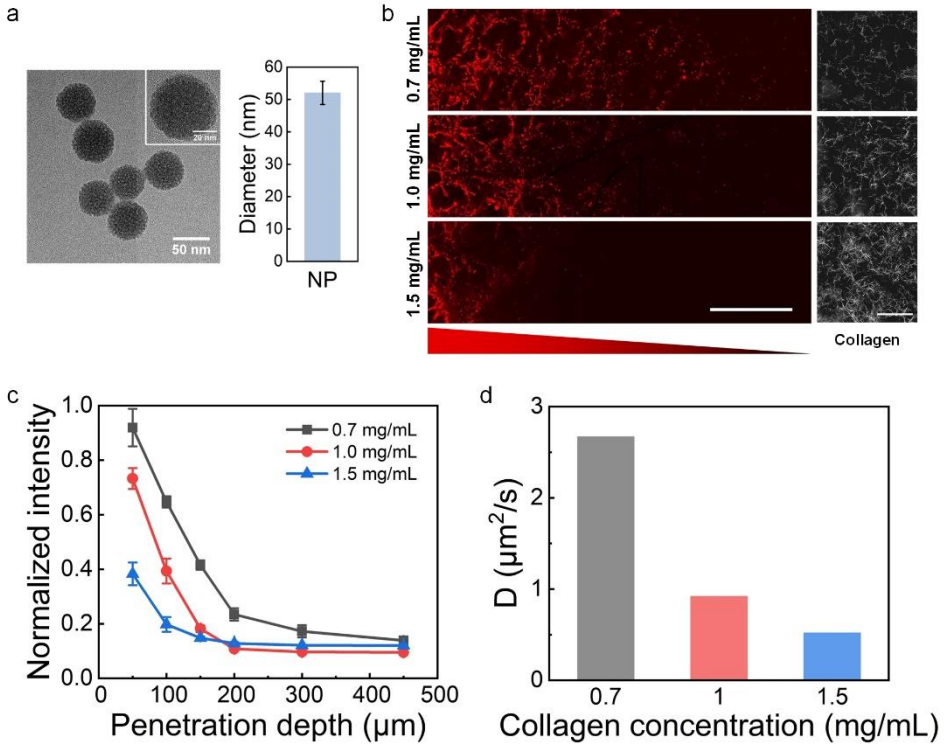

Fig. S3. Effect of collagen density on the diffusion of NPs with a size of 50 nm in collagen hydrogels. a, Representative TEM image of mesoporous silica NPs with a size of approximately 50 nm. Statistical analysis reveals the average diameter (N=20). **b,** Representative confocal images of channels with increasing collagen density. Reflectance images in the right panel show the morphology of the collagen hydrogels. (Scale bars, 100 μm) **c,** Penetration depth profile of NPs at t = 2 h in collagen hydrogels with increasing density. **d,** Effect of collagen density on the diffusion coefficient of NPs inside collagen hydrogels.

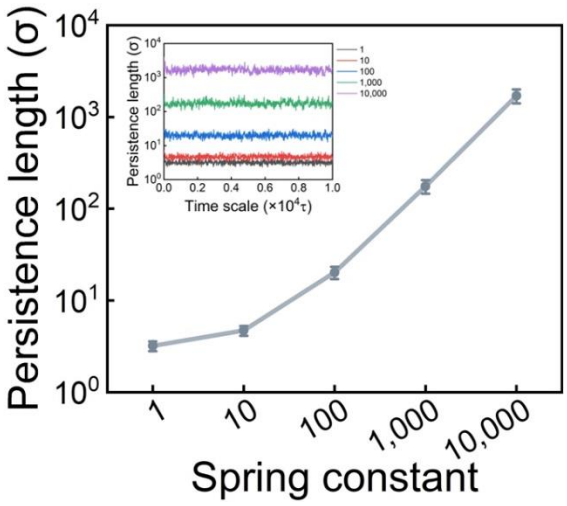

Fig. S4. The persistence length of polymer chains with increasing spring constants in the simulations.

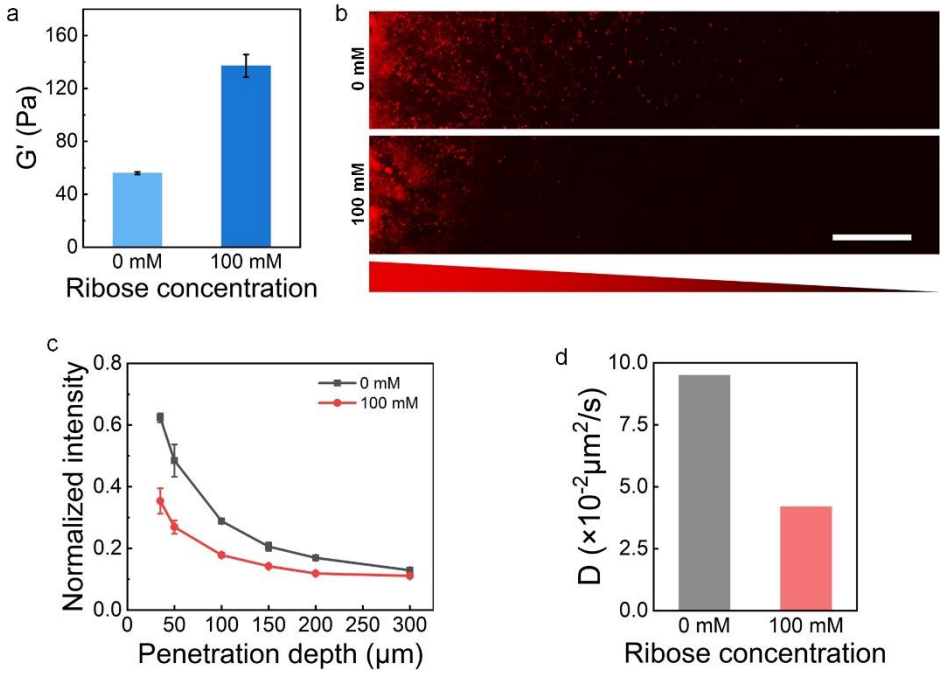

Fig. S5. Effect of collagen stiffness on the diffusion of NPs in collagen hydrogels. a, Increased stiffness of collagen by ribose glycation. **b,** Representative confocal images of NPs in collagen hydrogels with increased stiffness. (Scale bar, 50 μm) **c,** Penetration depth profile of NPs at t = 10 h in collagen hydrogels with increased stiffness. **d,** Effect of collagen hydrogel stiffness on the diffusion coefficient of NPs.

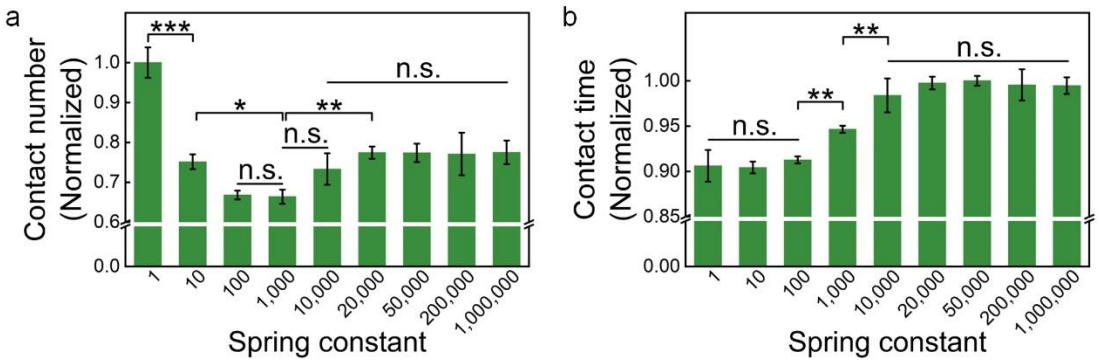

Fig. S6. The change of the contact number (a) and contact time (b) with the increase of the spring constant.

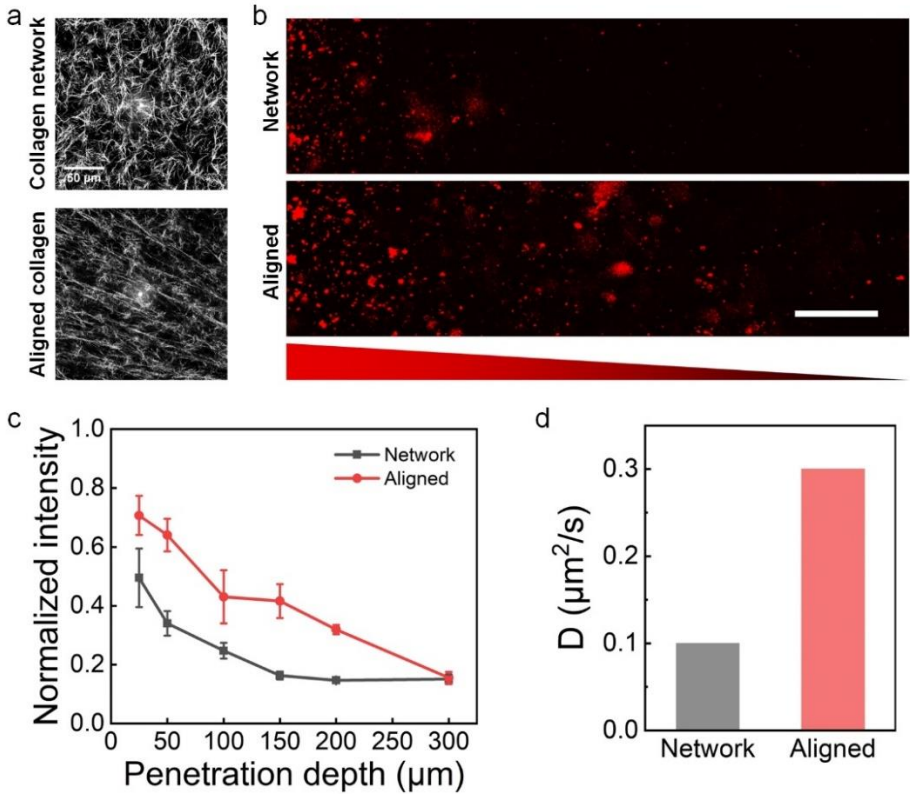

Fig. S7. Effect of collagen alignment on the diffusion of NPs in collagen hydrogels. a, Representative confocal reflectance images show the morphology of crosslinked collagen network and aligned collagen structure. **b,** Representative confocal fluorescence images of NPs in collagen hydrogels with original network and aligned structure. (Scale bar, 50 μm) **c,** Penetration depth profile of NPs at t = 6 h in collagen hydrogels with original network and aligned structure. **d,** Effect of collagen alignment on the diffusion coefficient of NPs.

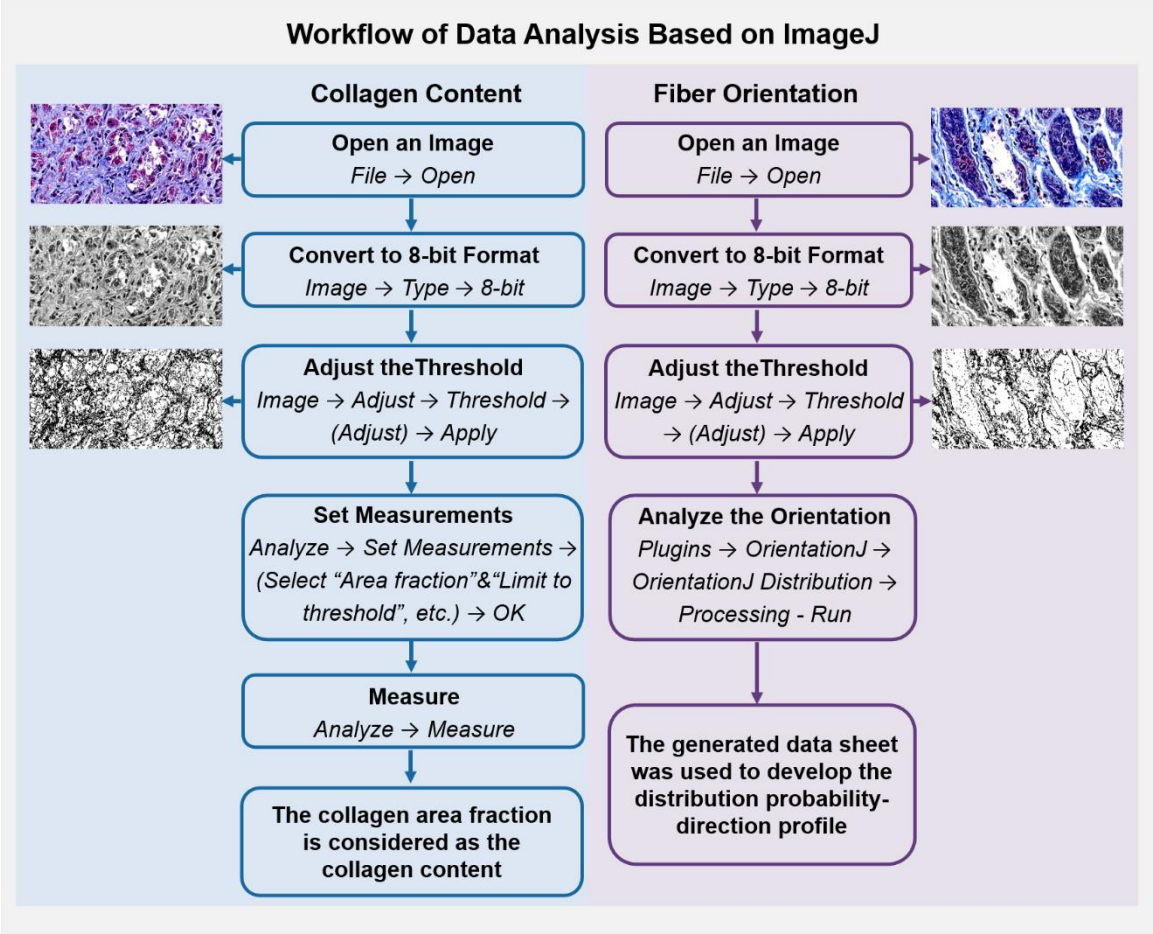

Fig. S8. Workflow of data analysis in ImageJ for Figure 2b and Figure 2c.

Tables

Table S1. Comparison of the size ratio in experiment and MD simulation and the calculated D_n (Diffusion coefficient in network), D_w (Diffusion coefficient in water) and D_r (Relative diffusion coefficient, D_n / D_w)

Experiment						
NP size	Collagen pore size		Size ratio (NP/Pore)	D_n ($\mu m^2/s$)	D_w ($\mu m^2/s$)	D_r
200 nm	0.5 mg/mL	~4 μm	1/20	0.92±0.18	~2.15	0.43±0.08
	1.0 mg/mL	~2.8 μm	1/14	0.59±0.13		0.27±0.06
	2.0 mg/mL	~2 μm	1/10	0.35±0.08		0.16±0.04
MD simulation						
NP size	Network pore size		Size ratio (NP/Pore)	D_n ($\times 10^{-2}\sigma^2/\tau$)	D_w ($\times 10^{-2}\sigma^2/\tau$)	D_r
2.5 σ	50 σ		1/20	0.42±0.05	~0.65	0.65±0.08
	36 σ		1/14.4	0.20±0.03		0.31±0.05
	24 σ		1/9.6	0.12±0.03		0.18±0.05

Table S2. Comparison of the crosslinked and aligned network model.

Density	Chain numbers		Distance between adjacent chains	
	Crosslinked	Aligned	Crosslinked	Aligned
4σ	972	961	4σ	2.4σ
6σ	432	441	6σ	3.6σ
8σ	243	256	8σ	4.8σ

Table S3. The ECM characterization values from references [2-4].

Cancer Types	Breast Cancer							Gastric Cancer	
Classification	Cancer Progression			Cancer Subtypes				Cancer Progression	
	Normal	DCIS	IDC	Luminal A	Luminal B	Her2+	TNBC	Normal	Cancer
Density	4	13	26	30	33	45	55	7	28
Stiffness	1	4-10 folds		3.1	3.7	6	5.8	221	1041
Alignment	~0.1-~0.35 (Anisotropic region proportion)							0.2	0.267

Table S4. Interaction parameters for different bead types.

Type1	Type2	Interaction	$k_b(\varepsilon/\sigma^2)$	$r_0(\sigma)$
NP	NP	Harmonic spring	200	0.47
Polymer	Polymer		23	1.0

Type1	Type2	Interaction	$\varepsilon_{lj}(\varepsilon)$	$b(\sigma)$	$r_c(\sigma)$
NP	NP	LJ Potential	0.01	0.5	2.0
NP	Polymer		0.1	1.0	5.0
Polymer	Polymer		0.1	0.5	2.0

References

1. Raeesi, V. and W.C. Chan, *Improving nanoparticle diffusion through tumor collagen matrix by photo-thermal gold nanorods.* Nanoscale, 2016. **8**(25): 12524-12530.
2. Acerbi, I., et al., *Human breast cancer invasion and aggression correlates with ECM stiffening and immune cell infiltration.* Integrative Biology Quantitative Biosciences from Nano to Macro, 2015(10): 1120.
3. Mercatelli, R., et al., *Collagen ultrastructural symmetry and its malignant alterations in human breast cancer revealed by polarization-resolved second-harmonic generation microscopy.* Journal of Biophotonics, 2020. **13**(8): e202000159.
4. Zhou, Z. H., et al., *Reorganized Collagen in the Tumor Microenvironment of Gastric Cancer and Its Association with Prognosis.* Journal of Cancer, 2017. **8**(8): 1466-1476.

Movie captions

Movie S1. NP diffusion in crosslinked network with mesh size of 4σ and spring constant of 100.

Movie S2. NP diffusion in crosslinked network with mesh size of 14σ and spring constant of 100.

Movie S3. NP diffusion in crosslinked network with mesh size of 4σ and spring constant of 10,000.

Movie S4. NP diffusion in aligned network with mesh size of 8σ and spring constant of 100.